

Noncovalent interaction between Ubc9 and SUMO promotes SUMO chain formation

Puck Knipscheer¹, Willem J van Dijk¹,
Jesper V Olsen², Matthias Mann²
and Titia K Sixma^{1,*}

¹ Department of Molecular Carcinogenesis, The Netherlands Cancer Institute and Center for Biomedical Genetics, Plesmanlaan, Amsterdam, The Netherlands and ²Department of Proteomics and Signaltransduction, Max-Planck Institute for Biochemistry, Am Klopferspitz, Martinsried, Germany

The ubiquitin-related modifier SUMO regulates a wide range of cellular processes by post-translational modification with one, or a chain of SUMO molecules. Sumoylation is achieved by the sequential action of several enzymes in which the E2, Ubc9, transfers SUMO from the E1 to the target mostly with the help of an E3 enzyme. In this process, Ubc9 not only forms a thioester bond with SUMO, but also interacts with SUMO noncovalently. Here, we show that this noncovalent interaction promotes the formation of short SUMO chains on targets such as Sp100 and HDAC4. We present a crystal structure of the noncovalent Ubc9–SUMO1 complex, showing that SUMO is located far from the E2 active site and resembles the noncovalent interaction site for ubiquitin on UbcH5c and Mms2. Structural comparison suggests a model for poly-sumoylation involving a mechanism analogous to Mms2-Ubc13-mediated ubiquitin chain formation.

The EMBO Journal (2007) 26, 2797–2807. doi:10.1038/sj.emboj.7601711; Published online 10 May 2007

Subject Categories: proteins; structural biology

Keywords: E2; crystal structure/poly-sumoylation; SUMO; Ubc9

Introduction

SUMO is a ubiquitin-related post-translational modifier that plays an important role in many cellular pathways including transcriptional regulation, intracellular transport, DNA repair and replication (Hoege *et al.*, 2002; Pichler and Melchior, 2002; Girdwood *et al.*, 2003; Seeler and Dejean, 2003; Stelter and Ulrich, 2003; Yang *et al.*, 2003; Muller *et al.*, 2004). Sumoylation of substrates generally functions by modulating their interaction properties with other proteins. Although SUMO has been detected mostly as single molecule modification, recent reports show that formation of SUMO chains is also observed for SUMO1 *in vitro* (Pichler *et al.*, 2002; Pedrioli *et al.*, 2006; Yang *et al.*, 2006) and for SUMO2/3 both *in vitro* and *in vivo* (Tatham *et al.*, 2001; Fu *et al.*, 2005).

*Corresponding author. Department of Molecular Carcinogenesis, The Netherlands Cancer Institute, Plesmanlaan 121, 1066 CX Amsterdam, The Netherlands. Tel.: +31 20 5121959; Fax: +31 20 5121954; E-mail: t.sixma@nki.nl

Received: 30 November 2006; accepted: 13 April 2007; published online: 10 May 2007

The process of SUMO modification is chemically similar to that of ubiquitin conjugation and the enzymes involved are mostly homologous. This involves the ligation of the C-terminus of the modifier to a lysine residue on the substrate, mediated by a highly regulated three-step cascade. For SUMO, this requires Aos1-Uba2 as E1 or activating enzyme, Ubc9 as E2 or conjugating enzyme and an E3 ligase such as PIAS, Pc2 or RanBP2 (Melchior, 2000; Johnson, 2004), although for many targets the cognate E3 has not yet been identified. In the first step, a thioester bond is formed between the modifier and the catalytic cysteine of the E1 enzyme in an ATP-dependent reaction. This thioester bond is subsequently transferred to the catalytic cysteine of the E2 enzyme, and in the last step the modifier is ligated to the ε-amino group of a lysine on the substrate with or without the help of an E3 ligase. In contrast to ubiquitin conjugation, the E2 enzyme in sumoylation plays an active role in target recognition by interacting with a ΨKxE/D consensus site sequence present on most, but not all targets (Sampson *et al.*, 2001).

The process uses one of four vertebrate SUMO isoforms that have partially overlapping target specificity. SUMO2 and SUMO3 differ only by three N-terminal residues and they share 45% sequence identity with SUMO1. The recently identified SUMO4 is more similar to SUMO2/3 (87%) than to SUMO1 (41%). Most of the SUMO1 in cells is found in conjugates, whereas there is a large pool of free cellular SUMO2/3 (Saitoh and Hinchev, 2000; Tatham *et al.*, 2001; Ayaydin and Dasso, 2004). Apparently, only SUMO2/3 form chains on substrates *in vivo*, whereas SUMO1 chains have only been shown *in vitro* (Pichler *et al.*, 2002; Pedrioli *et al.*, 2006; Yang *et al.*, 2006). The SUMO2/3 chains are linked through lysine 11, located in a traditional SUMO consensus motif in the flexible N-terminus of SUMO2/3 and seem to play a role in PML localization (Fu *et al.*, 2005). The single yeast SUMO homologue, Smt3, also forms chains *in vivo*, which are important for the regulation and assembly of the synaptonemal complex during meiosis (Bylebyl *et al.*, 2003; Cheng *et al.*, 2006).

Transient interaction is an important feature of the sumoylation process and here the E2, Ubc9, plays a central role by interacting with the E1, SUMO, the E3 and the target at various stages. Structural studies have revealed the nature of interaction of Ubc9 with a target (Bernier-Villamor *et al.*, 2002) and with an E3 enzyme (Reverter and Lima, 2005). Mutational analysis has indicated the interface between Ubc9 and the SUMO E1 to be mainly through its N-terminal helix and the loop between the first and the second β-strand (Bencsath *et al.*, 2002). This would suggest a similar interaction, as was recently shown for another ubiquitin-like molecule, Nedd8, with its E1 APPBP1-UBA3 (Huang *et al.*, 2005).

Ubc9 interacts with SUMO both in the thioester intermediate, a complex that has been structurally characterized for several ubiquitin E2s with ubiquitin (Hamilton *et al.*, 2001; McKenna *et al.*, 2003b), as well as in a noncovalent manner.

This noncovalent Ubc9–SUMO interaction involves the N-terminal helix of Ubc9, as well as the loop between this helix and the first β -strand, a surface that is also partially used for E1 interaction (Liu *et al*, 1999; Bencsath *et al*, 2002; Tatham *et al*, 2003). As a consequence, SUMO and the E1 can compete directly for interaction with the E2 (Bencsath *et al*, 2002). The role of the noncovalent interaction between SUMO and Ubc9 is unclear and functional studies have been complicated by this shared interaction site. The noncovalent binding between E2 and modifier is not unique for SUMO, as ubiquitin can also interact noncovalently with some of its E2 enzymes. The details of this interaction were recently shown for ubiquitin bound to UbcH5c (Brzovic *et al*, 2006) and to the E2 variant enzyme Mms2 (Brzovic *et al*, 2006; Lewis *et al*, 2006). The E2 variant Mms2 is thought to position ubiquitin for formation of lysine 63-linked chains of ubiquitin by the E2, Ubc13. The noncovalent interface of UbcH5c is also important for chain formation, but this is thought to follow a different mechanism.

Here, we show the crystal structure of the noncovalent complex between SUMO1 and Ubc9. SUMO1 interacts with its β -sheet with a consecutive stretch in Ubc9, connecting the first helix and strand. This site is located distant from the active site cysteine and resembles the Mms2 and UbcH5c ubiquitin noncovalent interfaces. We show that both SUMO1 and SUMO2 interact with Ubc9 similarly. The high-resolution structure enabled us to identify Ubc9 and SUMO mutants that specifically inhibit the interaction between the two proteins. These mutants were used to show that interference with this noncovalent interaction does not affect SUMO thioester formation, but instead strongly reduces SUMO2 chain formation on several targets. A model is presented in which the noncovalent interaction between SUMO and Ubc9 mediates SUMO chain formation, involving a mechanism similar to K63-linked ubiquitin chain formation by the Mms2-Ubc13 heterodimer.

Results

Crystal structure of noncovalent Ubc9–SUMO complex

To get insight in the functional importance of the noncovalent interaction between Ubc9 and SUMO, we solved the crystal structure of this complex using human Ubc9 and SUMO1 lacking the flexible N-terminal 20 amino acids (SUMO Δ N20) (Table I). Ubc9–SUMO crystals were grown by mixing the two components in a hanging-drop crystallization setup. The quality of the crystals allowed high-resolution data collection, after which the structure was solved by molecular replacement using the structures of Ubc9 (Tong *et al*, 1997) and SUMO1 (Pichler *et al*, 2005) as search models. The crystal structure shows that noncovalent interaction of SUMO1 with Ubc9 occurs on the backside of Ubc9 with respect to the active site cysteine (Figure 1A).

Complex formation does not cause large conformational changes in either Ubc9 or SUMO. Compared to previous crystal structures the r.m.s.d. is 0.79 Å for SUMO (using the core 77 C α atoms) and 0.60 Å for Ubc9 (using all C α atoms). The interface between the two proteins buries 727 Å² of solvent-accessible surface area on Ubc9 and 642 Å² on SUMO. This interface is relatively hydrophilic, with five salt bridges, eight direct hydrogen bonds and another 12 hydrogen bonds mediated through defined water molecules, but there

Table I Data collection and refinement statistics

	Ubc9 ^a SUMO covalent
<i>Data collection</i>	
Space group	P2 ₁
a, b, c (Å)	49.5, 35.0, 72.9
α , β , γ (°)	90, 93.41, 90
Resolution (Å)	50–1.4 (1.48–1.4) ^a
R_{sym}	6.0 (22.7)
$I/\sigma I$	6.3 (1.6)
Completeness (%)	99.2 (99.3)
Redundancy	3.5 (3.1)
<i>Refinement</i>	
Resolution (Å)	50–1.4
Number reflections	49 557
$R_{\text{work}}/R_{\text{free}}$	14.0/17.7
<i>Number of atoms</i>	
Protein	2130
Ligand/ion	1 Na ⁺
Water	408
B-factors	14.8
Protein	12.5
Ligand/ion	24.6
Water	26.8
<i>r.m.s.d.</i>	
Bond lengths (Å)	0.014
Bond angles (deg)	1.554

^aHighest resolution shell is shown in parenthesis.

are also many van der Waals interactions. On the Ubc9 side, all the residues involved in the interaction are situated in one continuous stretch of sequence at the end of the N-terminal helix, the first β -strand and the intervening loop (Figure 1B and E). This compact region of Ubc9 interacts with three of the five β -strands in SUMO's β -sheet. This is primarily β -strand 5 of SUMO, but also β -strand 1 and 3 and the loops connecting these strands are involved in the interface (Figure 1B and F). Details of the interactions are presented in Figure 1C and Supplementary Figure 1.

We compared our Ubc9–SUMO structure with the noncovalent complexes of ubiquitin with the E2 enzyme UbcH5c and the E2 variant Mms2, both determined by NMR (Brzovic *et al*, 2006; Lewis *et al*, 2006). Although UbcH5c and Ubc9 are only 36% identical, they both show the E2-specific α/β -fold and superimpose with an r.m.s.d. of 2.5 Å using 136 C α atoms. The E2 variant Mms2 is only 15% identical to Ubc9 and adopts an E2-like fold lacking the C-terminal helix. It superimposes on Ubc9 with an r.m.s.d. of 1.9 Å using 115 C α atoms. Secondary structures of ubiquitin and SUMO bound to the E2(-like) proteins are also highly similar, even though their sequence is only 18% conserved (r.m.s.d. 1.4 Å using 75 or 72 C α atoms for ubiquitin bound to UbcH5c and Mms2, respectively). Roughly, the interaction sites of ubiquitin on UbcH5c and SUMO1 on Ubc9 are conserved, both ubiquitin and SUMO1 interact with the backside of the E2, at least 20 Å away from the active site cysteine, and both use their β -sheet for this interaction. Also, the solvent-accessible surface area buried in the complexes is comparable, such as for Mms2-Ub, this is 641 Å² and 650 Å², respectively, and for UbcH5c-Ub, it is 567 Å² and 556 Å² (Figure 1E). If we superpose only the E2s, it becomes clear that the relative orientations of the modifiers are slightly different (Figure 1D and E). SUMO1 is rotated 28.4° towards the N-terminal helix of Ubc9, compared

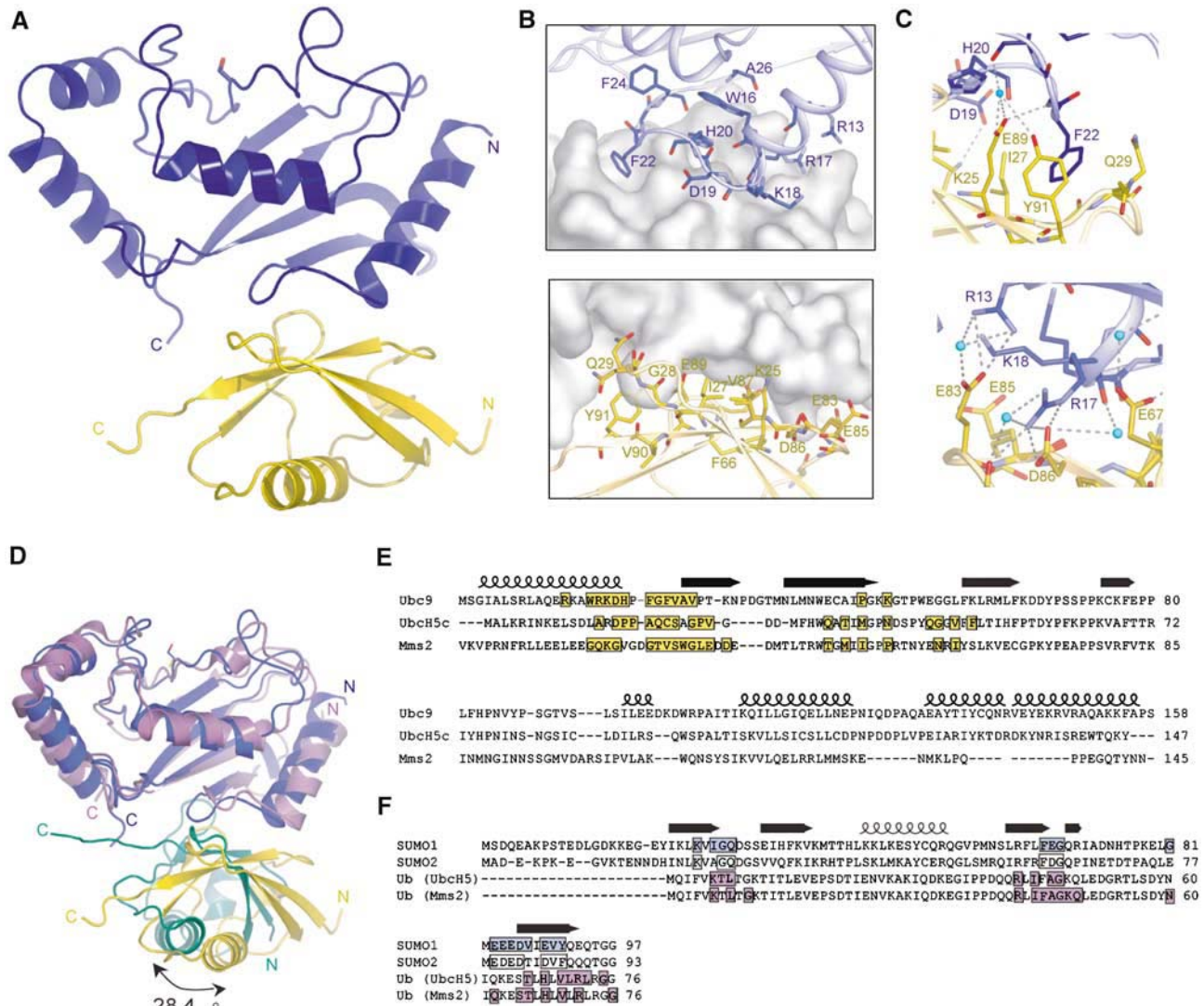


Figure 1 Structure of noncovalent Ubc9-SUMO1 complex. (A) Cartoon representation of the Ubc9-SUMO1 crystal structure, Ubc9 in blue and SUMO1 in yellow. The catalytic residue is shown in sticks. (B) Details of the interaction site. Residues of Ubc9 (upper panel) and SUMO1 (lower panel) involved in the interaction shown in sticks, counterpart shown as surface representation. (C) Close-up of Ubc9-SUMO1 interaction. (D) Superposition of the UbcH5c-Ubiquitin complex (purple and green, respectively) and the Ubc9-SUMO1 complex. Only UbcH5c and Ubc9 were used for the superposition, the angle between ubiquitin and SUMO is indicated. (E) Sequence alignment of Ubc9, UbcH5c and Mms2 showing secondary structure elements of Ubc9. Residues that loose at least 20% of their solvent accessible surface area upon complex formation with SUMO/ubiquitin are shown on a yellow background. (F) Sequence alignment of SUMO1, SUMO2 and ubiquitin with secondary structure elements of SUMO1 on top. Residues of SUMO1 involved in Ubc9 interaction (determined as in (E)) are shown on a blue background and homologous residues in SUMO2 are framed. Residues of ubiquitin involved in UbcH5c or Mms2 interaction have a purple background.

to ubiquitin on UbcH5c. The tilting of the ubiquitin in the Mms2 structure is 27.7°, compared to the SUMO, but only 14.4° if we compare it with ubiquitin interacting with UbcH5c (Figure 1D). Although crystal contacts could be involved, we did see the same orientation for SUMO in a second crystal form (data not shown). The difference in the position of the modifiers results in a change of interaction surfaces on the E2s, where SUMO interacts with Ubc9 mainly N-terminally, the ubiquitin interaction surface on UbcH5c and Mms2 is shifted somewhat towards the C-terminus (Figure 1E).

SUMO1 and SUMO2 interact with Ubc9 with similar affinities

Both SUMO1 and SUMO2 bind noncovalently to Ubc9 (Tatham *et al*, 2003) and even though they are only 44%

identical, the residues in the interface with Ubc9 are relatively well conserved (nine identical, four homologous, three different) (Figure 1F). Of the three nonconserved residues, Gly 81 (Glu 77 in SUMO2) only makes main chain contacts, and the other two, changing Ile 27 into an alanine (Ala 23 in SUMO2) and Val 87 into a threonine (Thr 83 in SUMO2) can be accommodated in the interface without problems. Therefore, we deduce that the interaction mode of Ubc9 with SUMO1 and 2 are likely to be very similar, in agreement with NMR studies of this interface (Liu *et al*, 1999; Tatham *et al*, 2003).

To determine the affinity of the interaction between Ubc9 and SUMO1 and 2, we used isothermal calorimetric analysis. In isothermal calorimetry (ITC), the absorbance or release of energy of mixing two components that interact with each

other can be measured as heat changes. These changes in heat can be used to determine the binding constant and thermodynamic parameters of the interaction. For the interaction between Ubc9 and SUMO1, we determined a K_d of 82 ± 23 nM (Figure 2A). The heat exchange or enthalpy contribution to the binding is relatively small (maximally 6 kcal/mol under these conditions), but high enough to calculate the K_d accurately. Previously, a slightly higher dissociation constant of 250 ± 70 nM has been reported for the Ubc9–SUMO1 interaction using ITC (Tatham *et al*, 2003). The only obvious differences in K_d measurement between ours and Tatham *et al* (2003) are a small pH difference (pH = 8.0 versus 7.5, respectively) and the presence of an N-terminal His-tag on Ubc9 in their experiments. Both of these factors could contribute to the threefold difference in K_d . When we performed identical ITC measurements replacing SUMO1 for SUMO2, we were not able to measure any reproducible heat exchange during the measurement. Nevertheless, if we collected the sample from the flow cell after the experiment and run it on an analytical gel filtration column, we observe complete complex formation between SUMO2 and Ubc9 (data not shown). As the heat exchange of the reaction for SUMO1 binding was very small, it seems likely that for SUMO2 the enthalpic contribution is even smaller and the reaction is mostly entropically driven, and can therefore not be measured by ITC.

For a direct comparison of the affinities of Ubc9 with SUMO1 and SUMO2, we therefore used an analytical gel filtration shift experiment. First, we tested the method using high protein concentrations by mixing pure samples of Ubc9 (50 μ M) and an excess of SUMO1 or SUMO2 (100 μ M) in 25 μ l, incubation at 4 °C for 10 min before running it on a Superdex 75 gel filtration column. Both for SUMO1 (Figure 2B, upper panel) and SUMO2 (Figure 2B, lower panel), all of the Ubc9 were shifted to the Ubc9–SUMO

complex peak, whereas the excess of SUMO eluted in a peak overlapping with the free SUMO peak. To compare affinities, we used lower concentrations of Ubc9 (390 nM) with varying SUMO concentrations, followed by gel filtration chromatography and Western blotting of the fractions using a Ubc9 antibody. This allowed visualization of the free Ubc9 peak shifting to the SUMO-bound peak upon increased SUMO concentrations in the samples (Figure 2C). Both SUMO1 and SUMO2 are able to shift the Ubc9 peak under these conditions and the peak shift occurs at similar SUMO1 and SUMO2 concentrations indicating similar affinities of Ubc9 for SUMO1 and SUMO2.

Ubc9H20D and SUMO1E67R inhibit noncovalent interaction

Although several groups have reported the noncovalent interaction between Ubc9 and SUMO, the function of this interaction has been subject of speculation. Based on mutant analysis, it has been proposed that the interaction is needed for SUMO thioester formation (Tatham *et al*, 2003). However, as the binding sites for SUMO and the E1 on Ubc9 partially overlap, it was difficult to create interface mutants that do not affect E1 interaction, and consequently, thioester formation. Now, based on our high-resolution structure, we searched for Ubc9 or SUMO1 mutants that only abolish the noncovalent interaction between Ubc9 and SUMO.

For SUMO1, we generated the following mutants: E67R, G68Y, V87W and E89R. These mutants were tested for their ability to interact with Ubc9 noncovalently, as well as for their activity in E1 and Ubc9 thioester formation. As summarized in Table II, all of these mutants showed decreased noncovalent interaction with Ubc9 and SUMOE67R, as well as SUMOE89R and SUMOV87W, were completely unable to interact with Ubc9 in the analytical gel filtration assay

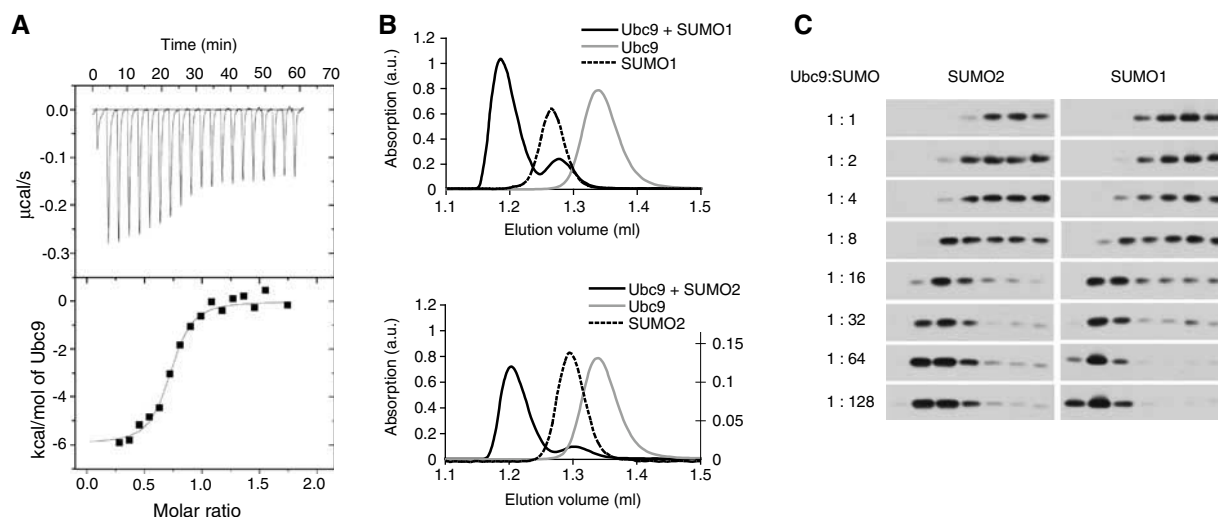


Figure 2 SUMO1 and SUMO2 have similar affinity for Ubc9. **(A)** Isothermal calorimetry data for noncovalent interaction between Ubc9 and SUMO1. Raw (upper panel) and processed (lower panel) data for 7 μ M SUMO titrated with 12 μ l injections of 70 μ M Ubc9. Processed data points were fitted to a model describing a single set of binding sites. Thermodynamic parameters for the interaction are $\Delta H = -5.96 \pm 0.2$ kcal/mol and $-\Delta TS = -3.87$ kcal/mol **(B)** Chromatograms of analytical gel filtration runs for Ubc9 with SUMO1 (upper panel) and Ubc9 with SUMO2 (lower panel). Runs of single proteins contained 60 μ M Ubc9 or 300 μ M SUMO1/2, complex runs contained 50 μ M Ubc9 and 100 μ M SUMO1/2. Ubc9–SUMO2 chromatogram has been scaled (see second y-axis) because SUMO2 contains few aromatic residues and therefore has low signals. **(C)** Gel-filtration-based shift assays visualized by Western blot analysis using anti-Ubc9. For SUMO2 (left panel), as well as for SUMO1 (right panel), several gel-filtration runs were performed with a constant Ubc9 and increasing SUMO concentrations (molar ratio is depicted on the left). Seven consecutive fractions ranging in elution volume from 1.15 to 1.4 ml are loaded on the gel for both SUMO1 and SUMO2.

(Supplementary Figure 2 and data not shown). SUMOE89R and V78W, however, were also impaired in either E1 or Ubc9 thioester formation or both, and were therefore not good candidates to study the function of the Ubc9–SUMO noncovalent interaction (Figure 3A and Supplementary Figure 2). The SUMOE67R mutant only has a minor defect in Ubc9 thioester formation and would, from these mutants, be the best candidate to study the role of noncovalent Ubc9–SUMO interaction (Figure 3B and Supplementary Figure 2).

For Ubc9, we tested mutations in four residues, R17E, H20D, G23R, and V25W and V25R (Table III). These mutants were tested for SUMO1 interaction and, in addition, for their ability to interact noncovalently with the E1, as well as their activity in Ubc9~SUMO thioester formation (Figure 3A and Supplementary Figure 2, data not shown). Valine 25 is equivalent to serine 22 in UbcH5c, mutating this residue inhibited noncovalent interaction with ubiquitin (Brzovic *et al*, 2006). In Ubc9, however, mutation of this residue did not affect the noncovalent binding of SUMO probably due to the fact that it is less well buried in the Ubc9–SUMO interface (Supplementary Figure 2). Also, the G23R mutation did not abolish Ubc9–SUMO noncovalent interaction. In contrast, the R17E and H20D mutants do disturb the interface and are strongly inhibited in Ubc9–SUMO interaction (Figure 3D, Supplementary Figure 2). However, Ubc9R17E was also

deficient in E1 interaction and strongly reduced in Ubc9~SUMO thioester formation and was therefore excluded from further studies. Ubc9H20D was the only Ubc9 mutant that abolished the noncovalent interaction with SUMO (Figure 3D) without affecting thioester formation (Figure 3C), even though it does show a reduction in E1 interaction (Supplementary Figure 2C). This mutation is therefore suited for further analysis of the function of noncovalent interaction between Ubc9 and SUMO.

Noncovalent Ubc9–SUMO interaction promotes SUMO chain formation

In both Mms2 and in UbcH5c, the noncovalent interaction with ubiquitin is involved in ubiquitin chain formation (VanDemark *et al*, 2001; Brzovic *et al*, 2006). Therefore, we analyzed whether the noncovalent Ubc9–SUMO interaction was important for free SUMO chain formation. We compared the wild-type and the H20D mutant Ubc9, which has lost the noncovalent interaction. The Ubc9 variants were incubated with SUMO, E1 and ATP at 37°C and SUMO chain formation was followed in time (Figure 4A). Under these conditions, neither SUMO1 nor the SUMO2 K11R mutant, which has lost the SUMO consensus site, forms SUMO chains efficiently, in accordance with previous reports (Tatham *et al*, 2001). SUMO2WT, however, readily forms chains with Ubc9WT,

Table II Summary of SUMO mutant data

SUMO	WT	E67R	G68Y	V87W	E89R
Ubc9 binding	++ ^a	–	+/-	–	–
E1 thioester	++	++	+/-	++	–
Ubc9 thioester	++	+	–	+/-	–

^a ++ 90–100% of SUMO WT activity, +70–90% of WT activity, +/- 40–60% of WT activity, – 0–20% of WT activity.

Table III Summary of Ubc9 mutant data

Ubc9	WT	R17E	G23R	V25W	V25R	H20D
SUMO binding	++ ^a	–	++	++	++	–
E1 interaction	++	–	++	++	++	+/-
Ubc9 thioester	++	–	ND	ND	ND	++

^aAs is but for Ubc9 mutants.
ND: not determined.

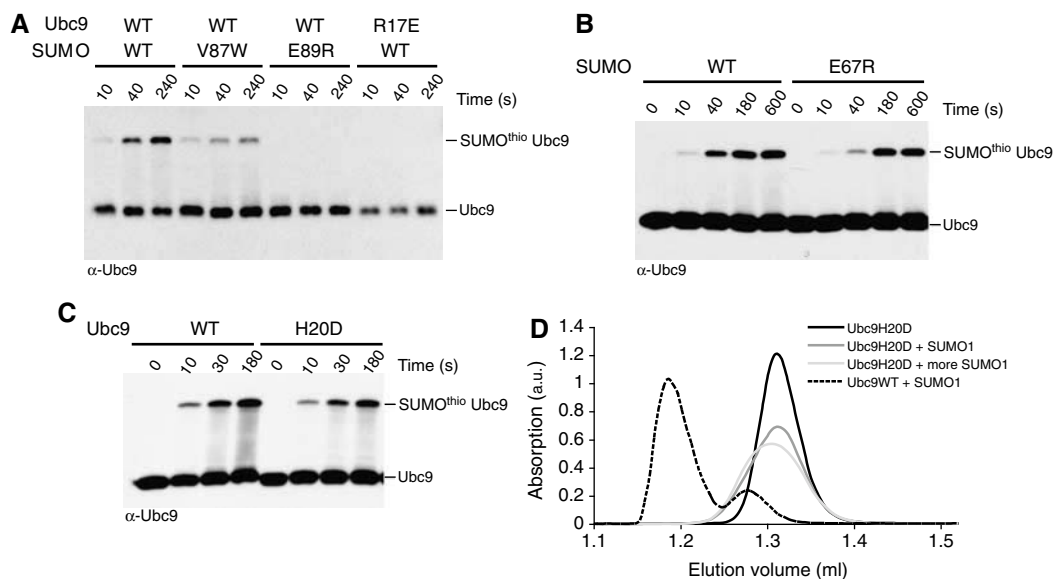


Figure 3 Mutants that interrupt noncovalent Ubc9–SUMO binding but not thioester formation. (A) Thioester formation followed in time for Ubc9 and SUMO1 wild type and mutants. Concentrations were: 100 nM E1, 900 nM Ubc9 and 3 μM SUMO1. (B) Thioester formation assay comparing SUMO1WT with SUMOE67R. Concentrations were: 200 nM E1, 1.4 μM Ubc9 and 15 μM SUMO1. (C) Thioester formation assay as in (B) comparing Ubc9WT with Ubc9H20D. (D) Noncovalent binding studied using analytical gel-filtration for Ubc9H20D with SUMO1. Curve indicated as ‘Ubc9 + SUMO1’ was 44 μM Ubc9H20D and 108 μM SUMO1, ‘Ubc9 + more SUMO1’ was 27 μM Ubc9H20D and 136 μM SUMO1. Free Ubc9H20D and the complex between Ubc9WT and SUMO are indicated for clarity.

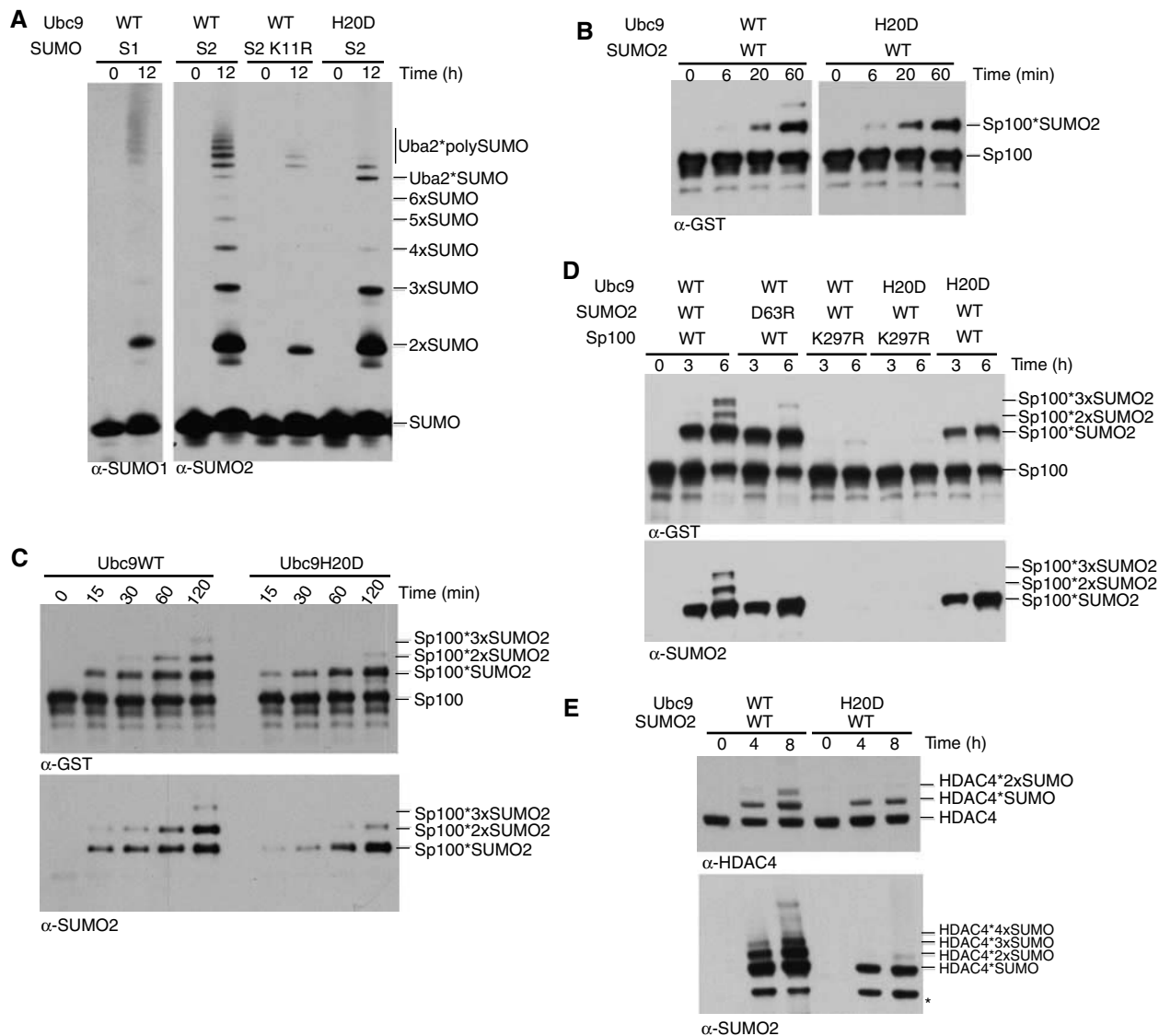


Figure 4 Noncovalent Ubc9-SUMO interaction promotes SUMO chain formation. (A) Free SUMO chain formation for SUMO1, SUMO2 and SUMO2K11R with Ubc9WT and Ubc9H20D. Formation of SUMO chains is followed in time using SUMO1 or SUMO2 antibodies as indicated. Concentrations were: 100 nM E1, 400 nM Ubc9 and 20 μ M SUMO. Note that Ubc9H20D is also strikingly different in forming higher order Uba2 conjugates that occur as a side effect of the reaction. Uba2 is a known target for sumoylation (Zhao *et al*, 2004; Hannich *et al*, 2005). The presence of SUMO-modified Uba2 was confirmed by mass spectrometry (data not shown). (B) Sumoylation of Sp100 with SUMO2 comparing Ubc9WT with Ubc9H20D. Concentrations were: 830 nM GST-Sp100, 175 nM E1, 400 nM Ubc9 and 20 μ M SUMO2 and detection was with anti-GST. (C) SUMO chain formation on Sp100 with SUMO2, comparing Ubc9WT with Ubc9H20D. Concentrations are identical to (B), except E1 was 150 nM, formation of GST-Sp100*SUMO2 conjugates is followed in time using either a GST antibody (upper panel) or a SUMO2 antibody (lower panel). (D) SUMO chain formation on Sp100 comparing several mutant proteins. Concentrations were: 1.3 μ M GST-Sp100, 10 nM E1, 300 nM Ubc9 and 10 μ M SUMO and detection was with anti-GST or anti-SUMO2. (E) Assay as in (C) but using GST-HDAC4 as a target and an HDAC4 antibody for the upper panel.

but the Ubc9H20D mutant is clearly and reproducibly less productive in chain formation (Figure 4A). Thus, loss of the noncovalent interaction inhibits SUMO2 chain formation.

Next, we tested SUMO2 chain formation on a known SUMO target, the transcriptional regulator Sp100. If we stop the reaction after 1 h, we observe mostly monosumoylation of Sp100 and, importantly, this is equally efficient for Ubc9WT compared to Ubc9H20D (Figure 4B). However, at the latest time point in the Ubc9WT reaction, a higher, potentially Sp100*2 \times SUMO, band is appearing. To investigate whether this indicates SUMO chain formation, we performed a similar experiment, but extended the incubation

time. At later time points, we now observe several higher bands using Ubc9WT that do not appear if we use Ubc9H20D, shown on Western blots with either GST or SUMO2 antibodies (Figure 4C).

These higher order bands are not formed very efficiently and it was important to check whether the higher molecular weight bands are a result of SUMO2 chain formation, or monosumoylation on multiple sites in Sp100. Therefore, we analyzed the Sp100*SUMO2, Sp100*2 \times SUMO2 and Sp100*3 \times SUMO2 samples by mass spectrometry. In all samples, one major modification site in Sp100 was found at K297, the lysine that has previously been identified as the

SUMO modification site (Sternsdorf *et al*, 1997). In addition, a small fraction (<5%) of a minor site was modified (K387). This indicates that most of the higher order bands are due to chain formation of SUMO2. Mass spectrometric analysis identified primarily SUMO2 K11, and to a small extent K5, as the acceptor lysines on SUMO2 itself. As a control for chain formation, we performed a similar sumoylation reaction using less enzyme, comparing Sp100WT that has lost the SUMO consensus lysine at 297 (Sp100K297R). Under these conditions, we still observe SUMO2 chain formation on Sp100WT, whereas Sp100K297R is hardly modified (Figure 4D). Meanwhile, the consensus site on SUMO2 is also required for the chain formation, as the SUMO2 K11R mutant is also reduced in SUMO2 chain formation (Supplementary Figure 3). These results demonstrate that SUMO chains are formed on Sp100 via the consensus site lysine 297, and that SUMO2 uses primarily lysine 11 to make these chains.

To examine the importance of the noncovalent interaction between Ubc9 and SUMO2 for the formation of these chains, we tested the Ubc9H20D mutant in the same Sp100 chain formation assay. Figure 4C and D show that this mutant is impaired in SUMO2 chain formation on Sp100. To test whether the importance of the noncovalent binding site for poly-sumoylation is a target-specific effect we investigated SUMO2 chain formation on another well-known SUMO target, histone deacetylase 4 (HDAC4). Also with this target, we see a profound inhibition of SUMO chain formation upon disruption of the noncovalent interaction site between SUMO and Ubc9 (Figure 4E).

To verify if the loss of chain formation was really due to the lack of noncovalent interaction, we tested the SUMO2D63R mutant, which is the equivalent of the SUMO1E67R mutation. It inhibits SUMO2-Ubc9 noncovalent interaction, whereas it is still competent in Ubc9 thioester formation (data not shown). This SUMO mutant also inhibits poly-sumoylation of Sp100 (Figure 4D). As loss of noncovalent interaction due to mutation either on Ubc9 or on SUMO2 affects chain formation, this strongly suggests that noncovalent interaction between Ubc9 and SUMO2 promotes poly-sumoylation of Sp100.

Discussion

Here, we have presented the crystal structure of the noncovalent complex between Ubc9 and SUMO1. The resemblance of this structure with the noncovalent complex between ubiquitin and UbcH5c, as well as with the E2 variant Mms2 and ubiquitin, underlines the conservation of this interaction between homologous pathways. The UEV (ubiquitin conjugating enzyme variant) domain of Tsg101 (and VPS23) also interacts noncovalently with ubiquitin, but this interaction is different as it primarily uses a β -tongue motif formed by the extended first and second beta-strands and the loop between them (Sundquist *et al*, 2004).

NMR studies have been performed on the noncovalent interface between Ubc9 and SUMO1, 2 and 3 (Liu *et al*, 1999; Tatham *et al*, 2003), all indicating that the interaction site on Ubc9 is primarily formed by the N-terminal region of Ubc9. We have now shown the high-resolution details of this interaction and found that SUMO interacts with the N-terminal helix, the first β -strand and the intervening loop of Ubc9.

Recently, a model for the interaction between Ubc9 and SUMO3 was created by docking approaches in combination with NMR interaction data (Ding *et al*, 2005). In this model, the equivalent residues of SUMO3, compared to SUMO1 in our structure, interact with Ubc9. As SUMO2 and 3 are completely identical in the interacting residues, and as we have shown that SUMO1 and SUMO2 interact with Ubc9 with similar affinities, we can conclude that all SUMO isoforms interact with Ubc9 using the same interaction site and with similar affinities. With a K_d of ~ 80 nM, the interaction between SUMO and Ubc9 is relatively strong compared to the interaction between ubiquitin and UbcH5c with a K_d of ~ 300 μ M (Brzovic *et al* 2006), and between ubiquitin and Mms2 with a K_d of ~ 100 μ M (McKenna *et al*, 2003a). Even though the buried surface areas between E2 and modifier are comparable in all three structures, there are more hydrogen bonds and salt bridges in the Ubc9-SUMO interface, which might account for the difference in affinity.

Two mutations, one in Ubc9 (H20D) and one in SUMO (E67R in SUMO1 or D63R in SUMO2), were identified that individually interfere with Ubc9-SUMO noncovalent interaction. These mutants enabled us to show that the interaction between Ubc9 and SUMO promotes SUMO chain formation on both Sp100 and HDAC4. There are several possible mechanisms that can explain the role of this interaction in chain formation. The simplest one would be that one Ubc9 molecule interacts with two SUMO molecules and the noncovalently bound SUMO acts as a direct acceptor for the thioester bound SUMO (donor). This mechanism is not likely, as the distance from the N-terminus of the acceptor SUMO to the active cysteine is too long to bridge the distance to the acceptor lysines K5 or K11, even if the N-terminal residues adopt an extended conformation.

Another possibility is that chain formation occurs by a mechanism similar to what has been proposed for UbcH5c (Brzovic *et al*, 2006). In that case, the noncovalent interaction between ubiquitin and UbcH5c is promoting large assemblies of activated UbcH5c \sim ubiquitin, which are required for processive BRCA1-directed ubiquitination. However, in our hands, the Ubc9 \sim SUMO thioester is not forming these large assemblies (data not shown) and even though we cannot completely rule out that higher order assemblies are formed with low affinity we do not favor this mechanism.

Our favored hypothesis, however, is that the polysumoylation that we observe involves a mechanism that follows the well-established model for ubiquitin chain formation, as seen in Mms2-Ubc13-dependent K63 polyubiquitination. This idea is based on structural comparison of Ubc9-SUMO with Mms2-ubiquitin and data of its interaction with ubiquitin-loaded Ubc13. In this last complex, the E2 variant (Mms2) can bind an acceptor ubiquitin noncovalently and form a heterodimer with a functional E2 (Ubc13) that is activated with ubiquitin. Modeling as well as structural studies have shown that in this complex the K63 of the acceptor ubiquitin is in close proximity to the activated cysteine of Ubc13, providing a mechanism for K63-linked ubiquitin chain formation (VanDemark *et al*, 2001; McKenna *et al*, 2003b; Lewis *et al*, 2006). The recently published crystal structure of the Ubc13 \sim Ub intermediate in complex with Mms2 also shows this quaternary complex, as it has a

ubiquitin molecule from a neighboring complex bound to the acceptor ubiquitin site on Mms2 (Figure 5A; Eddins *et al*, 2006).

A complex like this could also be formed between two identical E2s, which would require the E2 to interact with itself. Although Ubc9 is not a homodimer in solution, self-interaction has been shown in yeast two-hybrid systems (Hateboer *et al*, 1996; Kovalenko *et al*, 1996). If we superpose the Ubc9-SUMO complex on Mms2 bound to ubiquitin from the Mms2-Ubc13~Ub structure, a free Ubc9 on Ubc13, and SUMO on the thioester ubiquitin (Eddins *et al*, 2006), we can create a model that resembles the Mms2/Ubc13/2 × Ubiquitin complex (Figure 5B). In this model, we see that, although SUMO does not have a lysine at the equivalent position to K63 in ubiquitin, the N-terminus of the noncovalently bound SUMO is close to the active site of the adjacent Ubc9. For SUMO2, there are 14 residues of N-terminal tail that are not present in the structure, and the K11 and K5 could both easily reach the active site of the donor Ubc9. This attractive model provides a possible explanation why chain formation takes place on the N-terminal tail of SUMO2 and why the noncovalent interaction between Ubc9 and SUMO promotes this chain formation.

The chain formation that has been observed for SUMO2 (Tatham *et al*, 2001; Cheng *et al*, 2006) is less processive than that which has been seen for ubiquitin. This lower processivity is most likely an intrinsic feature of Ubc9 and not due to the *in vitro* reaction conditions, as polyubiquitin chains are easily formed *in vitro*, whereas the SUMO chains remain shorter. However, SUMO chains have not been extensively studied *in vivo* and, as the yeast homologue of SUMO, Smt3, seems to be able to form long chains *in vivo* (Bylebyl *et al*, 2003), it would be likely that additional factors are required for processive SUMO chain formation. This has also been shown for the ubiquitin system, where for example PCNA requires the E3 Rad18 for monoubiquitination and another E3, Rad5 for polyubiquitination. Similar to the requirement for a specific ubiquitin E3-ligase, the SUMO chain formation could also require a specialized E3 for chain formation.

Here, we presented data to show that the noncovalent interaction between Ubc9 and SUMO is important for SUMO chain formation. Structural comparisons led to a model analogous to the K63-type chain formation in ubiquitin chain formation. Interestingly, the affinity of Ubc9 for SUMO is much higher than that of Mms2 for ubiquitin. Conversely, the affinity of Ubc13 for Mms2 is much higher than that of Ubc9

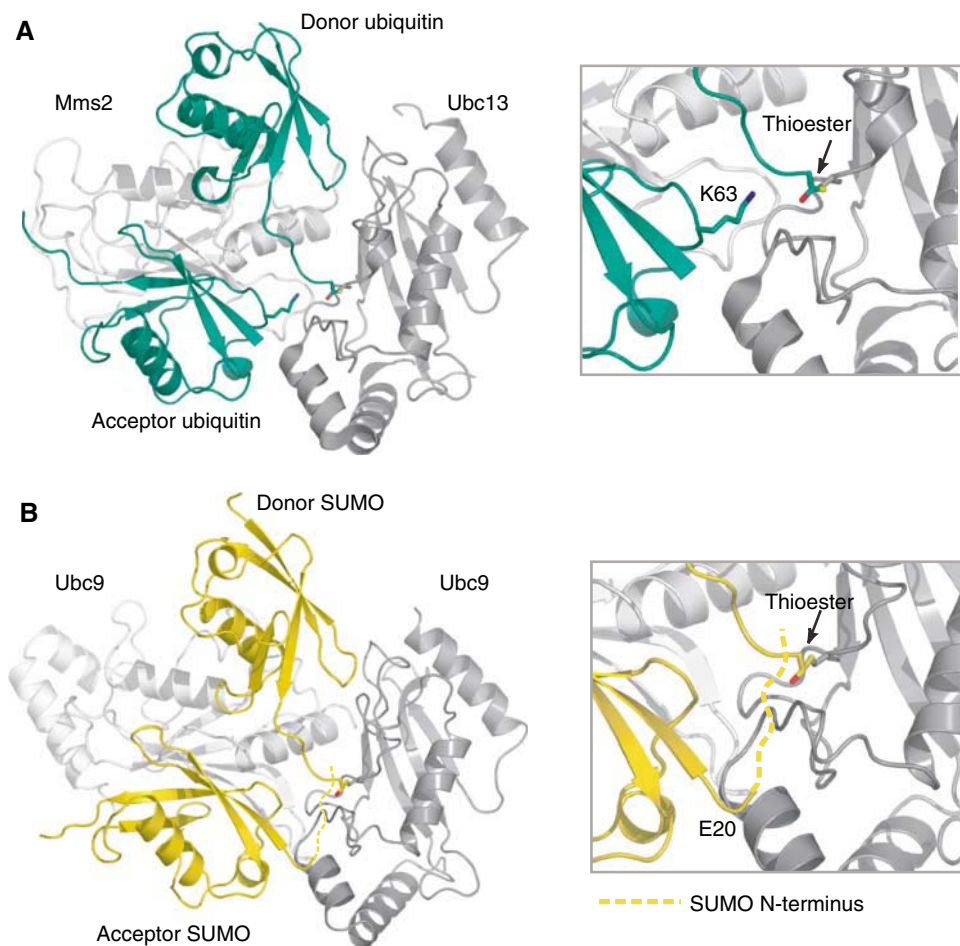


Figure 5 A model for SUMO chain formation. (A) K63 ubiquitin chain formation by the Mms2-Ubc13 heterodimer (Eddins *et al*, 2006) (PDB-code: 2GMI). Close-up shows Mms2 K63 in sticks and the Ubc13 thioester active site. (B) Structural model for SUMO chain formation. The noncovalent Ubc9-SUMO1 complex was superposed on Mms-Ub and another Ubc9 molecule was superposed on Ubc13 (A). Thioester SUMO was modeled by superposition on ubiquitin replacing the C-terminal tail with the one from ubiquitin. Close-up shows acceptor SUMO N-terminus and donor SUMO-Ubc9 thioester active site. Dotted line represents the N-terminal tail of SUMO that is not present in the structure.

for itself. Thus, in the two systems, the balance of affinities is maintained in different ways, emphasizing that ubiquitin and SUMO are analogous, but not identical. Nevertheless, the actual mechanism for chain formation seems once again surprisingly similar between the ubiquitin and SUMO pathways.

Materials and methods

Plasmids and antibodies

Ubc9, SUMO1(Δ N20), Aosl-Uba2 (Pichler *et al*, 2005), GST-Sp100 (Seeler *et al*, 2001) and GST-HDAC4 (Kirsh *et al*, 2002) were described before. Ubc9 and SUMO1 mutants were generated by site-directed mutagenesis. Mouse α -SUMO1 was obtained from Santa Cruz and Zymed and goat α -GST from Amersham. Goat α -Ubc9 and goat α -SUMO2 were kindly provided by F Melchior (Georg-August University, Göttingen). Secondary antibodies were from Biorad or Biosource.

Protein expression and purification

Purification of Ubc9, Aosl-Uba2, GST-Sp100, GST-HDAC4 was performed as described previously (Pichler *et al*, 2002; Pichler *et al*, 2005) and SUMO2 were expressed in BL21(DE3) cells using IPTG induction overnight at 15°C. Purification was performed on a Superdex 75 column in 20 mM Tris (pH 8.0), 100 mM NaCl, 0.1 mM PMSF, 1 mM DTT followed by an anion exchange (monoQ) column.

Analytical gel filtration

Protein-protein interaction studies by analytical gel filtration were performed on a Superdex 75 column on the SMART system (Pharmacia) in a buffer containing 20 mM Tris (pH 8.0) and 100 mM NaCl. Concentrations as indicated in the figure legends were mixed and incubated for 10 min at 4°C before loading (25–50 μ l) on the column. Eluted fractions were run on SDS-PAGE and either analyzed by coomassie staining, or by Western blot analysis using an antibody against Ubc9.

Isothermal titration calorimetry

ITC experiments were performed with the VP-ITC Micro Calorimeter (MicroCal Inc.) at 30°C. Stock solutions of Ubc9 and SUMO were prepared by dialysis of the purified proteins against a buffer containing 20 mM Tris (pH 8.0) and 5 mM β -mercaptoethanol at 4°C and were degassed before use. The sample cell (1.4 ml) contained SUMO (5–10 μ M), which was titrated with Ubc9 (50–100 μ M) using 12 μ l injections. The injections after saturation were used to determine the background signal. Corrected data were analyzed using software supplied by the ITC manufacturer to calculate the dissociation constant (K_d). Parameters were obtained for a model describing one set of binding sites, using nonlinear least-squares fitting.

Native gel shift assays

Interaction of SUMO E1 with Ubc9WT and mutants was determined by a native gel mobility shift assay. Ubc9 was incubated with increasing amounts of E1 for 15 min at room temperature. Bound and unbound forms were separated on a 6 or 8% polyacrylamide gel (acrylamide:bis, 29:1) in a Tris-Glycine buffer. Bands were visualized on a Western blot with anti-Ubc9.

E1 thioester formation

E1 thioester formation was performed at 8°C in the same buffer as the thioester formation. Aosl-Uba2 (3 μ M) was mixed with SUMO (22 μ M) and reactions were started by addition of 5 mM ATP. Samples from indicated time points were denatured in nonreducing loading buffer, run on SDS-PAGE and stained with Coomassie.

In vitro thioester formation and target sumoylation assays

Ubc9WT and mutant thioester formation assays were performed at 30°C in buffer containing 20 mM Tris (pH 8.0), 100 mM NaCl, 5 mM MgCl₂ and 0.1 mM DTT. Reactions contained Aosl-Uba2, SUMO and Ubc9 in concentrations as indicated in the figure legends. Reactions were started by addition of 5 mM ATP and at the indicated time points samples were denatured in nonreducing loading buffer.

Samples were run on SDS-PAGE, immunoblotted and analyzed with α -Ubc9.

Target sumoylation and free SUMO chain formation assays were performed at 37°C in buffer containing 20 mM HEPES (pH 7.3), 110 mM potassium acetate, 2 mM magnesium acetate, 0.05% Tween 20, 0.2 mM ovalbumin and 1 mM DTT. Reaction mixture contained Aosl-Uba2, SUMO1 or SUMO2, Ubc9 and either Sp100 or HDAC4 in case of target sumoylation, in concentrations as indicated in the figure legends. After start of the reaction by the addition of 5 mM ATP, samples were taken at the indicated time points and mixed with denaturing and reducing sample buffer. Samples were run on 8% SDS gels or 4–12% NuPage gels (Invitrogen) and bands were visualized by immunoblotting against α -GST, α -SUMO1 or α -SUMO2.

Mass spectrometry

The protein bands containing GST-SP100 conjugated with several SUMO2 molecules were excised from an SDS-PAGE gel and subjected to in-gel reduction, alkylation, trypsin digestion and subsequent sample desalting and concentration, as described previously (Olsen *et al*, 2004). The resulting peptide mixture was analyzed by nano-HPLC-MS/MS using an Agilent 1100 nanoflow system connected to a hybrid linear ion trap orbitrap (LTQ-Orbitrap) mass spectrometer (Thermo Electron, Germany), equipped with a nanoelectrospray ion source (Proxeon Biosystems, Odense, Denmark), essentially as described previously (Olsen *et al*, 2005).

Crystallization, data collection and structure determination

Ubc9-SUMO(Δ N20) crystals were grown at 4°C by mixing equimolar amounts of Ubc9WT or Ubc9C93S and SUMO(Δ N20) (450 μ M each) in a hanging drop with a mother liquor consisting of 16.5% (w/v) PEG3350, 100 mM BisTris (pH 5.5) and 15% (w/v) glycerol. The complex crystallized using either Ubc9WT or Ubc9C93S, as large plates with a maximum of 400 μ M in their largest dimension. Cryoprotection was achieved by increasing the concentration of glycerol to 25% (w/v). Data were collected on a single Ubc9C93S-SUMO1 crystal in a separate high- and low-resolution data set at 100 K on European Synchrotron Radiation Facility beam line ID14-2 ($\lambda = 0.933$). Data were processed with MOSFLM and SCALA (Collaborative Computational Project 4, 1994).

The structure was solved by molecular replacement with the program Molrep (Collaborative Computational Project 4, 1994) using both Ubc9 (Tong *et al*, 1997, Protein Data Bank (PDB) code 1U9A) and SUMO (Pichler *et al*, 2005, PDB code 2BF8). Rebuilding was performed with ARP/wARP (Perrakis *et al*, 1999) and Coot (Emsley and Cowtan, 2004), and refinement was done with REFMAC (Collaborative Computational Project 4, 1994). Percentages of residues in the most favored, additionally allowed, generously allowed and disallowed regions of the Ramachandran plot were 93.5, 6.0, 0.5 and 0.0%, respectively. The model includes 408 water molecules and one sodium ion from the protein storage buffer. Crystallographic parameters are summarized in Table 1. Buried solvent-accessible surface areas between the molecules were calculated with the program Areaimol (Collaborative Computational Project 4, 1994) and contacts between Ubc9 and SUMO were analyzed with the program NCONT (Collaborative Computational Project 4, 1994).

All structure figures were generated using Pymol (<http://www.pymol.org>). Atomic coordinates and structure factors have been deposited to the PDB with accession code 2uyz.

Supplementary data

Supplementary data are available at *The EMBO Journal* Online (<http://www.embojournal.org>).

Acknowledgements

We thank the Sixma and Perrakis lab group members for discussions and sharing reagents and especially Patrick Celie for help with the ITC experiments. Our special thanks go to Frauke Melchior and Andrea Pichler, for discussion, sharing reagents and critical reading of the manuscript. This work was funded by NWO-Pionier, CBG and EU-Rubicon grants.

References

- Ayaydin F, Dasso M (2004) Distinct *in vivo* dynamics of vertebrate SUMO paralogs. *Mol Biol Cell* **15**: 5208–5218
- Bencsath KP, Podgorski MS, Pagala VR, Slaughter CA, Schulman BA (2002) Identification of a multifunctional binding site on Ubc9p required for Smt3p conjugation. *J Biol Chem* **277**: 47938–47945
- Bernier-Villamor V, Sampson DA, Matunis MJ, Lima CD (2002) Structural basis for E2-mediated SUMO conjugation revealed by a complex between ubiquitin-conjugating enzyme Ubc9 and RanGAP1. *Cell* **108**: 1908
- Brzovic PS, Lissounov A, Christensen DE, Hoyt DW, Kleit RE (2006) A UbcH5/ubiquitin noncovalent complex is required for processive BRCA1-directed ubiquitination. *Mol Cell* **21**: 873–880
- Bylebyl GR, Belichenko I, Johnson ES (2003) The SUMO isopeptidase Ulp2 prevents accumulation of SUMO chains in yeast. *J Biol Chem* **278**: 44113–44120
- Cheng CH, Lo YH, Liang SS, Ti SC, Lin FM, Yeh CH, Huang HY, Wang TF (2006) SUMO modifications control assembly of synaptonemal complex and polycomplex in meiosis of *Saccharomyces cerevisiae*. *Genes Dev* **20**: 2067–2081
- Collaborative Computational Project 4 (1994) The CCP4 suite: programs for protein crystallography. *Acta Crystallogr* **50** (Part 5): OAD/9
- Ding H, Yang Y, Zhang J, Wu J, Liu H, Shi Y (2005) Structural basis for SUMO-E2 interaction revealed by a complex model using docking approach in combination with NMR data. *Proteins* **61**: 1050–1058
- Eddins MJ, Carlile CM, Gomez KM, Pickart CM, Wolberger C (2006) Mms2-Ubc13 covalently bound to ubiquitin reveals the structural basis of linkage-specific polyubiquitin chain formation. *Nat Struct Mol Biol* **13**: 915–920
- Emsley P, Cowtan K (2004) Coot: Model-building tools for molecular graphics. *Acta Crystallogr* **60**: 2126–2132
- Fu C, Ahmed K, Ding H, Ding X, Lan J, Yang Z, Miao Y, Zhu Y, Shi Y, Zhu J, Huang H, Yao X (2005) Stabilization of PML nuclear localization by conjugation and oligomerization of SUMO-3. *Oncogene* **24**: 5401–5413
- Girdwood D, Bumpass D, Vaughan OA, Thain A, Anderson LA, Snowden AW, Garcia-Wilson E, Perkins ND, Hay RT (2003) P300 transcriptional repression is mediated by SUMO modification. *Mol Cell* **11**: 0 AD/4
- Hamilton KS, Ellison MJ, Barber KR, Williams RS, Huzil JT, McKenna S, Ptak C, Glover M, Shaw GS (2001) Structure of a conjugating enzyme-ubiquitin thiolester intermediate reveals a novel role for the ubiquitin tail. *Structure* **9**: 897–904
- Hannich JT, Lewis A, Kroetz MB, Li SJ, Heide H, Emili A, Hochstrasser M (2005) Defining the SUMO-modified proteome by multiple approaches in *Saccharomyces cerevisiae*. *J Biol Chem* **280**: 1911
- Hateboer G, Hijmans EM, Nooij JB, Schlenker S, Jentsch S, Bernards R (1996) mUBC9, a novel adenovirus E1A-interacting protein that complements a yeast cell cycle defect. *J Biol Chem* **271**: 25906–25911
- Hoeghe C, Pfander B, Moldovan GL, Pyrowolakis G, Jentsch S (2002) RAD6-dependent DNA repair is linked to modification of PCNA by ubiquitin and SUMO. *Nature* **419**: 1912
- Huang DT, Paydar A, Zhuang M, Waddell MB, Holton JM, Schulman BA (2005) Structural basis for recruitment of Ubc12 by an E2 binding domain in NEDD8's E1. *Mol Cell* **17**: 341–350
- Johnson ES (2004) Protein modification by SUMO. *Annu Rev Biochem* **73**: 355–382
- Kirsh O, Seeler JS, Pichler A, Gast A, Muller S, Miska E, Mathieu M, Harel-Bellan A, Kouzarides T, Melchior F, Dejean A (2002) The SUMO E3 ligase RanBP2 promotes modification of the HDAC4 deacetylase. *EMBO J* **21**: 2682–2691
- Kovalenko OV, Plug AW, Haaf T, Gonda DK, Ashley T, Ward DC, Radding CM, Golub EI (1996) Mammalian ubiquitin-conjugating enzyme Ubc9 interacts with Rad51 recombination protein and localizes in synaptonemal complexes. *Proc Natl Acad Sci USA* **93**: 2958–2963
- Lewis MJ, Saltibus LF, Hau DD, Xiao W, Spyropoulos L (2006) Structural basis for non-covalent interaction between ubiquitin and the ubiquitin conjugating enzyme variant human MMS2. *J Biomol NMR* **34**: 89–100
- Liu Q, Jin C, Liao X, Shen Z, Chen DJ, Chen Y (1999) The binding interface between an E2 (UBC9) and a ubiquitin homologue (UBL1). *J Biol Chem* **274**: 16979–16987
- McKenna S, Hu J, Moraes T, Xiao W, Ellison MJ, Spyropoulos L (2003a) Energetics and specificity of interactions within Ub.Uev.Ubc13 human ubiquitin conjugation complexes. *Biochemistry* **42**: 7922–7930
- McKenna S, Moraes T, Pastushok L, Ptak C, Xiao W, Spyropoulos L, Ellison MJ (2003b) An NMR-based model of the ubiquitin-bound human ubiquitin conjugation complex Mms2.Ubc13. The structural basis for lysine 63 chain catalysis. *J Biol Chem* **278**: 13151–13158
- Melchior F (2000) SUMO—nonclassical ubiquitin. *Annu Rev Cell Dev Biol* **16**: 591–626
- Muller S, Ledl A, Schmidt D (2004) SUMO: a regulator of gene expression and genome integrity. *Oncogene* **23**: 1915
- Olsen JV, de Godoy LM, Li G, Macek B, Mortensen P, Pesch R, Makarov A, Lange O, Horning S, Mann M (2005) Parts per million mass accuracy on an Orbitrap mass spectrometer via lock mass injection into a C-trap. *Mol Cell Proteomics* **4**: 2010–2021
- Olsen JV, Ong SE, Mann M (2004) Trypsin cleaves exclusively C-terminal to arginine and lysine residues. *Mol Cell Proteomics* **3**: 608–614
- Pedrioli PG, Raught B, Zhang XD, Rogers R, Aitchison J, Matunis M, Aebersold R (2006) Automated identification of SUMOylation sites using mass spectrometry and SUMOn pattern recognition software. *Nat Methods* **3**: 533–539
- Perrakis A, Morris R, Lamzin VS (1999) Automated protein model building combined with iterative structure refinement. *Nat Struct Biol* **6**: 458–463
- Pichler A, Gast A, Seeler JS, Dejean A, Melchior F (2002) The nucleoporin RanBP2 has SUMO1 E3 ligase activity. *Cell* **108**: 1911
- Pichler A, Knipscheer P, Oberhofer E, van Dijk WJ, Korner R, Olsen JV, Jentsch S, Melchior F, Sixma TK (2005) SUMO modification of the ubiquitin-conjugating enzyme E2-25 K. *Nat Struct Mol Biol* **12**: 264–269
- Pichler A, Melchior F (2002) Ubiquitin-related modifier SUMO1 and nucleocytoplasmic transport. *Traffic* **3**: 0 AD/6
- Reverter D, Lima CD (2005) Insights into E3 ligase activity revealed by a SUMO-RanGAP1-Ubc9-Nup358 complex. *Nature* **435**: 1902
- Saitoh H, Hinchey J (2000) Functional heterogeneity of small ubiquitin-related protein modifiers SUMO-1 versus SUMO-2/3. *J Biol Chem* **275**: 6252–6258
- Sampson DA, Wang M, Matunis MJ (2001) The small ubiquitin-like modifier-1 (SUMO-1) consensus sequence mediates Ubc9 binding and is essential for SUMO-1 modification. *J Biol Chem* **276**: 21664–21669
- Seeler JS, Dejean A (2003) Nuclear and unclear functions of SUMO. *Nat Rev Mol Cell Biol* **4**: 0 AD/9
- Seeler JS, Marchio A, Losson R, Desterro JM, Hay RT, Chambon P, Dejean A (2001) Common properties of nuclear body protein SP100 and TIF1alpha chromatin factor: role of SUMO modification. *Mol Cell Biol* **21**: 3314–3324
- Stelter P, Ulrich HD (2003) Control of spontaneous and damage-induced mutagenesis by SUMO and ubiquitin conjugation. *Nature* **425**: 1911
- Sternsdorf T, Jensen K, Will H (1997) Evidence for covalent modification of the nuclear dot-associated proteins PML and Sp100 by PIC1/SUMO-1. *J Cell Biol* **139**: 1621–1634
- Sundquist WI, Schubert HL, Kelly BN, Hill GC, Holton JM, Hill CP (2004) Ubiquitin recognition by the human TSG101 protein. *Mol Cell* **13**: 783–789
- Tatham MH, Jaffray E, Vaughan OA, Desterro JM, Botting CH, Naismith JH, Hay RT (2001) Polymeric chains of SUMO-2 and SUMO-3 are conjugated to protein substrates by SAE1/SAE2 and Ubc9. *J Biol Chem* **276**: 35368–35374
- Tatham MH, Kim S, Yu B, Jaffray E, Song J, Zheng J, Rodriguez MS, Hay RT, Chen Y (2003) Role of an N-terminal site of Ubc9 in SUMO-1, -2, and -3 binding and conjugation. *Biochemistry* **42**: 9959–9969
- Tong H, Hateboer G, Perrakis A, Bernards R, Sixma TK (1997) Crystal structure of murine/human Ubc9 provides insight into the variability of the ubiquitin-conjugating system. *J Biol Chem* **272**: 1922

- VanDemark AP, Hofmann RM, Tsui C, Pickart CM, Wolberger C (2001) Molecular insights into polyubiquitin chain assembly: crystal structure of the Mms2/Ubc13 heterodimer. *Cell* **105**: 711–720
- Yang M, Hsu CT, Ting CY, Liu LF, Hwang J (2006) Assembly of a polymeric chain of SUMO1 on human topoisomerase I *in vitro*. *J Biol Chem* **281**: 8264–8274
- Yang SH, Jaffray E, Senthinathan B, Hay RT, Sharrocks AD (2003) SUMO and transcriptional repression: dynamic interactions between the MAP kinase and SUMO pathways. *Cell Cycle* **2**: 0AD/11
- Zhao Y, Kwon SW, Anselmo A, Kaur K, White MA (2004) Broad spectrum identification of cellular small ubiquitin-related modifier (SUMO) substrate proteins. *J Biol Chem* **279**: 20999–21002